2017

Evaporation from a shallow, saline lake in the Nebraska Sandhills: Energy balance drivers of seasonal and interannual variability

Diego Andrés Riveros-Iregui
University of North Carolina at Chapel Hill, diegori@unc.edu

John Lenters
University of Wisconsin Madison, john.lenters@colorado.edu

Colin Peake
University of Nebraska-Lincoln, cspeake87@gmail.com

John T. Ong
University of Nebraska-Lincoln, jbong@huskers.unl.edu

Nathan C. Healey
NASA Jet Propulsion Laboratory, natehealey@hotmail.com

See next page for additional authors

Journal of Hydrology 553 (2017) 172–187

Contents lists available at ScienceDirect

Journal of Hydrology

journal homepage: www.elsevier.com/locate/jhydrol

Research papers

Evaporation from a shallow, saline lake in the Nebraska Sandhills: Energy balance drivers of seasonal and interannual variability

Diego A. Riveros-Iregui [a,*], John D. Lenters [b], Colin S. Peake [c], John B. Ong [d], Nathan C. Healey [e], Vitaly A. Zlotnik [d]

[a] Department of Geography, University of North Carolina at Chapel Hill, Chapel Hill, NC, USA
[b] University of Wisconsin-Madison, Boulder Junction, WI, USA
[c] School of Natural Resources, University of Nebraska-Lincoln, Lincoln, NE, USA
[d] Department of Earth and Atmospheric Sciences, University of Nebraska-Lincoln, Lincoln, NE, USA
[e] NASA Jet Propulsion Laboratory, California Institute of Technology, Pasadena, CA, USA

ARTICLE INFO

Article history:
Received 6 March 2017
Received in revised form 12 July 2017
Accepted 2 August 2017
Available online 4 August 2017

ABSTRACT

Despite potential evaporation rates in excess of the local precipitation, dry climates often support saline lakes through groundwater inputs of water and associated solutes. These groundwater-fed lakes are important indicators of environmental change, in part because their shallow water levels and salinity are very sensitive to weather and climatic variability. Some of this sensitivity arises from high rates of open-water evaporation, which is a dominant but poorly quantified process for saline lakes. This study used the Bowen ratio energy budget method to calculate open-water evaporation rates for Alkali Lake, a saline lake in the Nebraska Sandhills region (central United States), where numerous groundwater-fed lakes occupy the landscape. Evaporation rates were measured during the warm season (May – October) over three consecutive years (2007–2009) to gain insights into the climatic and limnological factors driving evaporation, as well as the partitioning of energy balance components at seasonal and interannual time scales. Results show a seasonal peak in evaporation rate in late June of 7.0 mm day^{-1} (on average), with a maximum daily rate of 10.5 mm day^{-1} and a 3-year mean July-September (JAS) rate of 5.1 mm day^{-1}, which greatly exceeds the long-term JAS precipitation rate of 1.3 mm day^{-1}. Seasonal variability in lake evaporation closely follows that of net radiation and lake surface temperature, with sensible heat flux and heat storage variations being relatively small, except in response to short-term, synoptic events. Interannual changes in the surface energy balance were weak, by comparison, although a 6-fold increase in mean lake level over the three years (0.05–0.30 m) led to greater heat storage within the lake, an enhanced JAS lake-air temperature gradient, and greater sensible heat loss. These large variations in water level were also associated with large changes in absolute salinity (from 28 to 118 g kg^{-1}), with periods of high salinity characterized by reductions in mass transfer estimates of evaporation rate by up to 20%, depending on atmospheric conditions and absolute salinity. Energy balance estimates of evaporation, on the other hand, were found to be less sensitive to variations in salinity. These results provide regional insights for lakes in the Nebraska Sandhills region and implications for estimation of the energy and water balance of saline lakes in similar arid and semi-arid landscapes.

1. Introduction

Saline, groundwater-fed lakes are important indicators of environmental change, in part because their size, water level, and salinity are very sensitive to weather and climate (Williams, 2002). In particular, open-water evaporation is typically a dominant component of the water budget for saline lakes, often greatly exceeding the average precipitation rate of the surrounding region (Winter, 1990, Winter et al., 2001). With little or no surface water outlet, saline lakes can also undergo disproportionately large changes in areal extent in response to small changes in precipitation, runoff, or evaporation (Micklin, 1992; Sahagian, 2000; Steenburgh et al., 2000). Langbein (1961) first hypothesized that the long-term balance of the salinity in a saline lake was mediated by its water level, which in turn was mediated by the long-term balance between water input and discharge by evaporation and often involved Aeolian salt dust removal (e.g., Zlotnik et al., 2012). Long-term monitoring of saline lakes is therefore crucial to determine seasonal patterns and to establish the relation among water levels, salinity,

* Corresponding author at: 327 Carolina Hall, Chapel Hill, NC 27599-3220, USA.
E-mail address: diegori@unc.edu (D.A. Riveros-Iregui).

http://dx.doi.org/10.1016/j.jhydrol.2017.08.002
0022-1694/

and evaporation rates. However, these intricate dynamics appear to be specific to each lake (Rimmer et al., 1999; Abbo et al., 2003), further substantiating the value of long-term observations.

Long-term observations in Lake Kinneret, a saline lake in the Jordan River watershed in Israel, have demonstrated that lake level plays an important role in the flux of solutes to the lake, especially at periods of high lake level (Rimmer and Gal, 2003). These researchers report a positive relation for both water and solute discharges with lake level, likely as a result of groundwater dynamics and high leaching of solutes during the rainy season. The influx of solutes is also positively correlated with rainfall on an annual basis (Rimmer and Gal, 2003). Similar observations, however, are rare throughout other saline lakes in the world and are particularly rare in the context of evaporation rates.

In North America, saline lakes play a prominent role in the landscape of the Great Plains region and, specifically, in the Nebraska Sandhills (NSH), the largest vegetated dune field in the western hemisphere and a critical recharge region for the High Plains and Ogallala aquifers (Scanlon et al., 2012). The NSH contain nearly 2000 interdunal lakes across an area of about 58,000 km^2 (Loope et al., 1995). The generally east-sloping landscape of the Sandhills includes a region of minimal slope in the west that contains shallow, endorheic or poorly draining, groundwater-fed lakes, many of which are saline (Bleed and Flowerday, 1998). Open-water evaporation is a dominant component of the energy and water balance of lakes in the NSH, yet most of the relevant research in this region has focused on evapotranspiration from dune areas (Billesbach and Arkebauer, 2012). As such, lake evaporation remains one of the most poorly quantified processes in climate and groundwater models for the NSH and similar regions (Chen and Hu, 2004; Evans et al., 2005; Radell and Rowe, 2008).

Understanding the role of evaporation in the energy, water, and solute balance of saline lakes first requires quantification of the relevant processes. Lake evaporation is commonly estimated using eddy covariance, mass transfer, or energy balance techniques. (For method comparison and review, see Drexler et al., 2004 and Rosenberry et al., 2007.) Among them, eddy covariance is an accurate, but intensive technique that is effective over a wide range of lake sizes, including large, deep lakes whose heat storage term would otherwise be difficult to quantify (Blanken et al., 2000, 2011). The Bowen ratio energy budget (BREB) method, on the other hand, has proven reliable for estimating lake evaporation from small lakes, so long as the heat storage term is properly quantified (Lenters et al., 2005; Winter et al., 2003). In addition, mass transfer techniques are often employed once one of the other two methods has been applied long enough to develop reliable transfer coefficients (Tanny et al., 2008; Liu et al., 2012; McGloin et al., 2014).

A few studies have used the BREB method in the NSH to estimate terrestrial evapotranspiration (ET), which has been shown to be much higher in wet, interdunal areas compared to upland dune areas (Billesbach & Arkebauer, 2012; Healey et al., 2011). These studies highlight the disproportionately higher water losses that occur in wet portions of the otherwise dry Sandhills landscape. These previous studies provide some insight into the regional energy and water balance of the *terrestrial* landscape in the NSH. To the best of our knowledge, however, no direct measurements of *open-water* evaporation have been reported for the NSH region, and limited understanding of such processes can be derived from previous studies of the much drier surrounding landscape.

Our objective here is to quantify and analyze open-water evaporation rates for a typical saline lake in the NSH. Using the BREB technique, we provide new insights into the climatic factors that drive lake evaporation and energy balance partitioning at seasonal and interannual time scales. Given the significant role that the NSH region occupies for one of the most agriculturally productive regions of the world, this information is necessary to constrain the primary drivers of water and solute balances and to accurately estimate evaporation and recharge rates across this region.

2. Methods

2.1. Site description

This study was conducted at Alkali Lake, a saline lake in the western margin of the Sandhills (41.82° N, −102.60° W; Fig. 1). Alkali Lake has a surface area of roughly 50 hectares that varies widely seasonally and annually. Lake area, depth, and volume are strongly controlled by temporal dynamics of the various water budget components. Among them, evaporation and groundwater in-seepage are dominant. According to existing classifications of lakes with substantial groundwater components to the water balance, it is a groundwater discharge lake (Zlotnik et al., 2010), as also clearly shown by geophysical techniques (Ong et al., 2010; Befus et al., 2012). Average water depth at Alkali Lake is 0.2 m, but ranges from 0.1 to 1.2 m. Overland flow entering the lake is limited, given the high permeability of the sandy soils and dunes that surround it. The lake water is dominated by sodium (Na) and potassium (K) anions and has been found in a previous study to have a pH of 10.4 and salinity ranging from 36.9 to 78.9 parts per thousand (McCarraher, 1977). Lake chemistry in the western Sandhills is largely influenced by evaporative concentration of groundwater (Bleed and Flowerday, 1998).

2.2. Instrumentation and monitoring

A buoy constructed from the hull of a Hobie Bravo catamaran sailboat (Hobie Cat Company, Oceanside, CA) was deployed near the center of Alkali Lake in June 2007 and remained on the lake for the duration of this study (2007–2009). Variables measured on the buoy include downward and upward shortwave radiation (pyranometer model CMP21, Kipp & Zonen, Delft, The Netherlands), downward and upward longwave radiation (pyrgeometer model CGR4, Kipp & Zonen, Delft, The Netherlands), air temperature and relative humidity (model HMP45C, Vaisala, Helsinki, Finland), electrical conductivity/salinity (multi-parameter sonde model YSI 600R, Fondriest, Fairborn, OH), two estimates of bulk surface water temperature (from the YSI 600R sonde and a HOBO U22-001, Onset, Bourne, MA), surface water "skin" temperature (model SI-111, Apogee, Logan, UT), barometric pressure (model CS100, Campbell Sci., Logan, UT), wind speed and direction (model 05106, RM Young Company, Traverse City, MI), and rainfall (model TE525MM, Texas Electronics, Dallas, TX).

All meteorological and YSI sonde variables at the buoy were sampled every 10 s using a data logger (model CR1000, Campbell Sci., Logan, UT), while bulk water temperature from the HOBO sensor was sampled every 10 min. Additionally, two pressure transducers (HOBO U20 Titanium Water Level Data Logger, Onset, Bourne, NA) were installed near the eastern and western ends of the lake to measure water level and temperature at 20-min intervals. An additional sonic-ranging water level gage was deployed on the buoy on June 29, 2009 to provide supplementary measurements of lake level (model SR50, Campbell Sci., Logan, UT). Locations of the instrumented buoy and pressure transducers are shown in Fig. 1. Bulk water temperature at the buoy was smoothed to hourly and 3-hourly (centered) running means in order to obtain more robust estimates of the daily change in lake heat content. The IRT-derived surface temperature measurements were used for any calculations that required measurements of the lake "skin" temperature (e.g., saturation vapor pressure and outgoing longwave radiation) and were carefully quality controlled through systematic intercomparison with the four independent sources of bulk

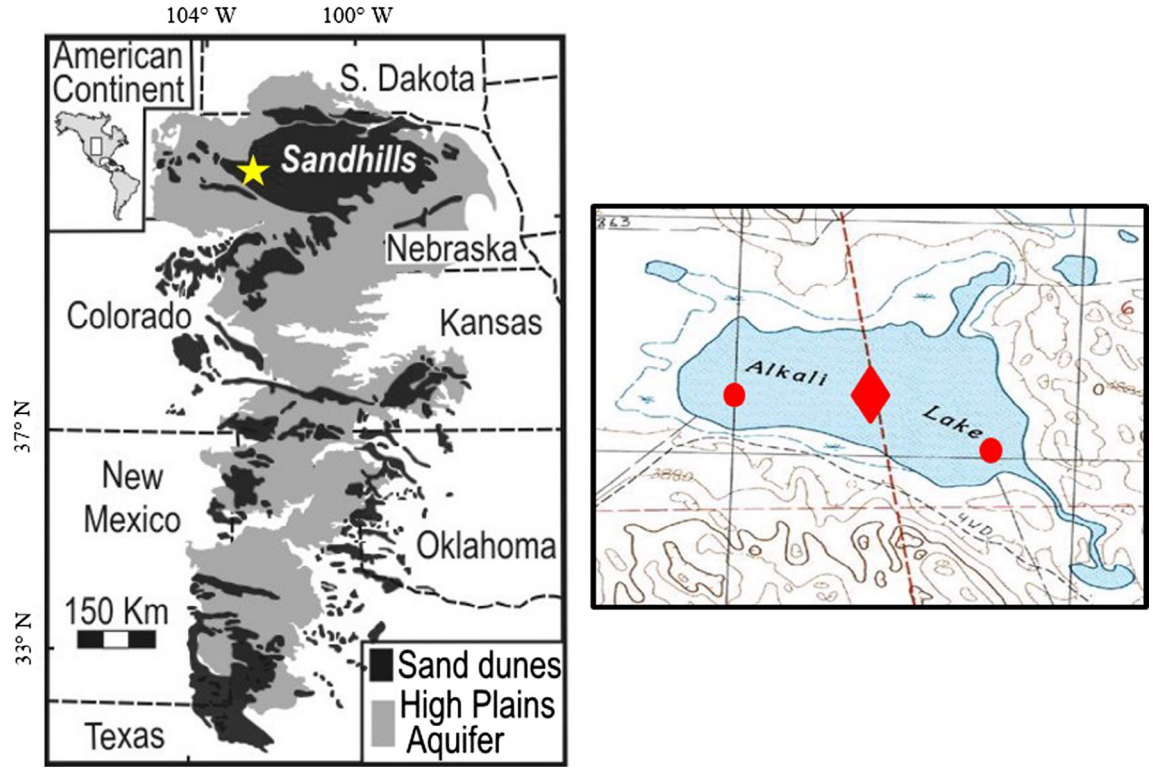

Fig. 1. Locations of the main hydrogeologic features of the study area, the High Plains Aquifer, the Nebraska Sandhills, and Alkali Lake. Red circles indicate the location of the water level sensors, while the diamond indicates the position of the instrumented buoy and water temperature/conductivity sensors. Modified from Ong (2010).

water temperature measurements. Aside from occasional data gaps due to power failure or instrument malfunction, energy balance measurements were available for all three years during the ice-free season (roughly May through October), with July-August-September (JAS) being the primary 3-month study period, characterized by largely gap-free data across all three years (2007–2009). Winter periods were not analyzed in this study due to frequent power failures, logistical constraints in accessing the site, and lack of ice cover and ice thickness measurements.

In addition to the instrumentation (described above) that was installed at Alkali Lake, environmental variables were also measured at a nearby station of the Automated Weather Data Network (AWDN), operated by the High Plains Regional Climate Center. Located ~50 km north of Alkali Lake, near Alliance, Nebraska (42.18 N, −102.92 W), the Alliance North weather station is the closest site to Alkali Lake and has a 25-year data record with hourly measurements of air temperature and humidity, wind speed and direction, solar radiation, and precipitation. Data from this weather station were used for general comparison purposes and for characterizing the longer-term climate variability in the region. For direct comparison with the Alkali Lake data, hourly observations from the AWDN station were also averaged to daily and 3-month means using JAS data from 2007 to 2009.

2.3. Energy balance and Bowen ratio measurements

The energy balance for a lake can be written as follows:

$$\bar{R}_{net} + \bar{Q}_{sed} + \bar{A}_{net} - (\overline{LE} + \bar{H}) = \Delta\bar{S}, \quad (1)$$

where $\bar{R}_{net}$ is net radiation, $\bar{Q}_{sed}$ is sediment heat flux, $\bar{A}_{net}$ is net heat advection, $\overline{LE}$ is the latent heat flux, $\bar{H}$ is sensible heat flux, and $\Delta\bar{S}$ is the rate of change in heat storage (Lenters et al., 2005); all components are reported in W m^{-2}, and the overbars indicate daily averages. Total daily evaporation was calculated for periods when complete BREB measurements were available (Jun 29, 2007 – Oct 14, 2007; May 12, 2008 – Oct 11, 2008; and Jun 28, 2009 – Nov 3, 2009). The common, gap-free time period that encompasses all three years is June 29 to October 11 (105 days).

Based on the shallow depth of Alkali Lake and numerous observations, surface temperature was found to be similar to the volumetric lake-mean temperature. We also determined from the water balance and groundwater temperatures that thermal advection term is likely to be much smaller than other components of the energy budget of Alkali Lake, allowing one to assume $A_{net} \approx 0$ (Lenters et al., 2005). More specifically, since Alkali Lake is a groundwater discharge lake, thermal advection comes mostly from cold, groundwater seepage. Advection from groundwater influx (A_{GI}) can be calculated from $A_{GI} = \rho_w\, c_w\, F_{GI}\, \Delta T_{GI}$, where ρ_w is the density of water (1000 kg m^{-3}), c_w is the specific heat of water (4186 J kg^{-1} °C^{-1}), F_{GI} is the groundwater influx (m s^{-1}), and ΔT_{GI} is the difference in temperature between the lake water and inflowing groundwater (Lenters et al., 2005). Average groundwater temperatures near Alkali Lake are ~12 °C, while summer lake temperatures range from 10.0 °C to 28.3 °C. The lake water balance reveals that groundwater in-seepage averages around 2.5 mm/day into Alkali Lake. Using the maximum temperature difference between lake water and groundwater (16.3 °C), this yields an average advective heat flux of only 1.8 W m^{-2}, which is considerably smaller than the primary energy budget components (e.g., net radiation). Large, daily values of thermal advection are possible but rare, and previous assumptions of negligible advection in shallow waters have also been shown to be valid (Parkhurst et al., 1998).

Neglecting the advection term, Eq. (1) is re-arranged for calculation of daily evaporation rates as follows:

$$\overline{LE} = \frac{\bar{R}_{net} - \Delta\bar{S} + \bar{Q}_{sed}}{1 + B} \quad (2)$$

where B is the Bowen ratio, or the ratio of sensible to latent heat flux (dos Reis and Dias,1998):

$$B = \frac{\bar{H}}{\overline{LE}} = \gamma \frac{\overline{U(T_s - T_a)}}{\overline{U(e_s - e_a)}} \quad (3)$$

Here, $\gamma = c_{pa}\ P/(0.622\ L_v)$ is the psychrometric constant (kPa °C^{1}), where c_{pa} is the specific heat of air (J kg^{-1} °C^{-1}), P is atmospheric pressure (kPa), and L_v is the latent heat of vaporization (J kg^{-1}). Other terms in Eq. (3) include wind speed (U, m s^{-1}), air temperature (T_a, °C), surface water temperature (T_s, °C), saturation vapor pressure at the surface water temperature (e_s, kPa), and atmospheric vapor pressure (e_a, kPa).

Net radiation is calculated as follows:

$$\bar{R}_{net} = (\bar{R}_{swd} - \bar{R}_{swu}) + (\bar{R}_{lwd} - \bar{R}_{lwu}) \quad (4)$$

where $\bar{R}_{swd}$, $\bar{R}_{swu}$, $\bar{R}_{lwd}$, and $\bar{R}_{lwu}$ are downward (incoming) shortwave, upward shortwave (i.e., reflected), downward (incoming) longwave, and upward longwave radiation, respectively, all of which were directly measured over the lake at the buoy location. Upward longwave radiation, which is comprised of both emitted and reflected components, can also be calculated from $\bar{R}_{lwu} = \varepsilon\sigma T_s^4 + (1-\varepsilon)\bar{R}_{lwd}$, where ε is the emissivity of water (0.97) and σ is the Stefan-Boltzman constant (5.67×10^{-8} W m^{-2} K^{-4}). The daily rate of change in lake heat storage, $\Delta\bar{S}$ is calculated from the following equation:

$$\Delta\bar{S} \approx \rho_w c_w \bar{h} \frac{\Delta\bar{T}}{\Delta t} \quad (5)$$

where ρ_w is the density of water, c_w is the specific heat of water, $\bar{h}$ is the daily mean lake depth, $\Delta\bar{T}$ is the daily change in bulk water temperature at the buoy (estimated from 3-h centered mean observations at 0:00h and 0:00h local time), and Δt = 86,400 s (i.e., one day).

In previous studies, the BREB technique has typically been applied at weekly or longer timescales, given the often large uncertainty in the lake heat storage term (Lenters et al., 2005). However, the very shallow depth of Alkali Lake (~0.3 m) allows us to implement the BREB technique at much shorter timescales, in part because of the 3-h running mean bulk water temperatures that are applied to help minimize uncertainty in the daily heat storage term. A thorough error analysis was also conducted to fully assess the level of uncertainty in the energy budget (see description below).

2.4. Sediment heat flux model

Sediment heat flux is often neglected for deep lakes (dos Reis and Dias, 1998; Oroud, 1997) or simplified to represent only the average annual cycle (Lenters et al., 2005; Winter et al., 2003). However, for shallow lakes in a strongly varying climate, the magnitude of the sediment heat flux can be comparable to or larger than the rate of heat storage in the water column. Thus, to quantify its contribution to the lake energy balance, we explicitly modeled sediment heat flux into and out of Alkali Lake using the one-dimensional heat flux equation for lakebed sediments (Keshari and Koo, 2007; Núñez et al., 2010; Smith, 2002):

$$\frac{\partial T_{sed}}{\partial t} = \alpha_s \frac{\partial^2 T_{sed}}{\partial z^2} \quad (6)$$

where T_{sed} is sediment temperature, T is the 3-h running mean bulk water temperature (at hourly timesteps, averaged across all three sites on the lake), α_s is the thermal diffusivity of the lake sediments (4.0×10^{-6} m^2 s^{-1}; based on *in situ* measurements using a Decagon KD2 Pro), and z (m) is the depth of the sediment layer.

Eq. (6) was solved numerically using an explicit finite difference scheme with upper and lower boundary conditions. The upper boundary condition is set by the hourly lake temperature forcing (over the full annual cycle), while the lower boundary condition assumes zero heat flux below 12 m, where temperature fluctuations become minimal. In fact, most of the sediment temperature variability was found to occur in the top 4 m of soil. The model was initialized by running ~13 years of spin-up, with the first 11 years forced by 2005 water temperature (i.e., 11 years in a row for 2005, followed by 2006–2009). Water temperature was estimated for the pre-observation period of 2005, 2006, and the first half of 2007 using a regression against local air temperature data (from June 2007 to November 2009). At the beginning of the simulation, the entire sediment matrix was initialized at a temperature of 11.64 °C, which is the average sediment temperature that the model converged to during the 2005 spin-up period. Using a thickness of 6 cm for each discrete lakebed layer and a constant thermal conductivity of 1.2 W m^{-1} K^{-1} (from *in situ* Decagon KD2 Pro measurements at various locations throughout the lake bed), the model was found to be stable during the spin-up and 2007–2009 observation periods.

The sediment heat flux into/out of the lake water column is numerically equal to the vertically integrated hourly rate of heat storage in the 12-m soil column:

$$Q_{sed} = \rho_{sed} c_{sed} \sum \frac{\partial T_{sed}}{\partial t} \partial z \quad (7)$$

Here, ρ_{sed} is the soil density (kg m^{-3}), c_{sed} is the specific heat of the sediments (J kg^{-1} K^{-1}), and $\rho_{sed}\ c_{sed}$ = 3.1×10^6 J m^{-3} K^{-1} is the volumetric heat capacity. Similar to the thermal diffusivity and conductivity, heat capacity was directly measured in the field using a Decagon KD2 Pro.

2.5. Salinity effects

The effects of salinity in modifying the heat capacity of the lake water and the water-air vapor pressure gradient were explicitly accounted for in this study. The water activity, a_w, is defined as the ratio of the saturation vapor pressure of water over a saline surface (e_s) to that of fresh water (e_s^*) and is always less than 1 (Oroud, 2001; Salhotra, 1985):

$$a_w = \frac{e_S}{e_S^*} = \gamma_w X_w \quad (8)$$

where γ_w is the activity coefficient of water and X_w is the mole fraction of water containing solute, calculated from

$$X_w = \frac{m_w}{m_w + \sum_{i=1}^{N} m_i} \quad (9)$$

In Eq. (9), m_w is the molality of water, m_i is the molality of the solute, and N is the number of constituent solutes. For dilute solutions obeying Raoult's Law, γ_w = 1 and $\alpha_w \approx X_w$ (Garrels and Christ, 1965). The salinity-corrected saturation vapor pressure, e_s, which is used in calculating the Bowen ratio and mass-transfer estimates of latent heat flux, can then be calculated from:

$$e_S = a_w e_S^* \quad (10)$$

Periodic water samples from Alkali Lake were analyzed in March 2009, March 2010, and October 2010 to assess the water chemistry and corroborate the buoy-based measurements of electrical conductivity (EC) and salinity. Water samples from neighboring lakes, wells, and streams were also collected to characterize the local water chemistry, including a broad range of EC values and water activity. Several empirical equations relating EC to water activity, density, salinity, and absolute salinity were then developed (Ong, 2010) and are listed in Table 1. Together with the continuous EC measurements from the YSI sonde at Alkali Lake

Table 1
Regression equations relating EC (x, in units of mS/cm) to activity of water, salinity, absolute salinity, and density (y values). Regressions are based on 27 different water samples. Also shown is an exponential regression equation relating lake level (z, in cm) to absolute salinity (y, in g/kg).

Variable	Regression equation	R^2
Activity of water, a_w	$y = -0.00057617x + 1.000$	0.99
Salinity (g/L)	$y = 1.255\ x$	0.99
Absolute salinity (g/kg)	$y = 1.186225\ x$	0.99
Density (kg/L)	$y = 0.000963916\ x + 0.996993$	0.99
Absolute salinity (g/kg)	$y = 119.47e^{-0.032672z}$	0.89

(deployed at a depth of 10–20 cm), these regressions were used to calculate daily values of water density, specific heat, and a_w as a function of time. The sonde was deployed from May 2008 to November 2009, covering two summers and a complete annual cycle. An empirical relationship between water level and absolute salinity was developed (Table 1; $R^2 = 0.89$) to fill data gaps in 2007, when sonde measurements were not available.

2.6. Mass transfer estimates of sensible and latent heat flux

The mass-transfer (MT) technique relates evaporation and sensible heat flux to the processes affecting the removal of water vapor and heat from the boundary layer above the air-water interface at the surface of a lake (Lee and Swancar, 1997). In general, higher wind speeds above the lake surface cause larger amounts of water vapor and heat to be transported away from the lake, as do increases in the lake-air vapor pressure gradient. Therefore, evaporation is generally related to wind speed and the vertical vapor pressure gradient, measured between the lake surface and a fixed reference height (typically 2 m). Similarly, sensible heat flux is typically proportional to wind speed and the lake-air temperature gradient.

MT-derived evaporation rates (E_{MT}) and sensible heat flux (H_{MT}) can be calculated as follows:

$$\overline{LE}_{MT} = N_E \overline{U}(e_s - e_a) \tag{11}$$

$$\overline{H}_{MT} = N_H \overline{U(T_s - T_a)} \tag{12}$$

where N_E is the transfer coefficient for latent heat flux, and N_H is the corresponding transfer coefficient for sensible heat flux. Best estimates of N_E and N_H in each equation typically come from a calibration between MT estimates of *LE* and *H* and similar estimates using the more accurate BREB technique (or eddy covariance measurements). Lee and Swancar (1997), for example, used this approach to determine a best-fit slope of $N_E = 0.0114$ for a seepage lake in Florida.

Some of the quantities in Eqs. (3), (11), and (12) involve cross products of wind speed and other variables, and unless the covariance among these variables is small, the cross products must be calculated prior to averaging (Brutsaert, 1982; Jobson, 1972; Kondo, 1972; Webb, 1960, 1964). This is particularly important for the diurnal cycle, since diurnal covariances between wind speed and air temperature, for example, can be substantial (Jobson, 1972; Kondo, 1972; Webb, 1960, 1964). Similar to Hage (1975), we explicitly account for covariances at diurnal (and longer) timescales by calculating the cross-product quantities in Equations (11) and (12) using hourly mean inputs, and then averaging the products to longer timescales (e.g., daily and seasonal means). Similarly, both the Bowen ratio (Eq. (3)) and shortwave albedo were calculated as the ratio of the mean numerator and mean denominator (rather than the mean of the ratio).

2.7. Data Collection and QA/QC

2.7.1. Solar radiation

Unexpectedly high or low values of shortwave albedo were occasionally noted in the buoy observations, which can occur as a result of wind, tilting of the buoy, and/or temporary shading of the pyranometer(s) by an obstruction. To correct for these errors, hourly outliers were assigned theoretical maximum or minimum albedo values (for both clear and cloudy conditions) based on a functional relationship with sun angle determined from data collected by Payne (1972). Roughly 16% of the daytime albedo values were reset using this approach. A second screening of the data was then performed using an on-site albedo/sun angle relationship based on the (corrected) *in situ* data collected at Alkali Lake. This resulted in an additional 14% of the daytime albedo values being adjusted (i.e., 30% total), mostly during the morning and evening hours, when sun angle is low. The overall effect of these corrections on the daily mean net shortwave radiation was not found to be large, primarily because incoming solar radiation is relatively weak during the morning and evening hours.

2.7.2. Lake level

Periodic staff gage measurements were made at Alkali Lake to assist in validating the automated lake level observations from the two pressure transducers (and the buoy-based sonic ranging sensor). Both pressure sensors showed similar daily variability to each other ($R^2 = 0.9$), but with a bias in one of the sensors that developed in 2009. This bias was corrected (using regressions with earlier time periods), and then the average water level from the two pressure transducers was compared with daily mean measurements from the sonic sensor during 2009. The two datasets were found to agree very well ($R^2 = 0.98$), with little bias during the 2009 period (RMSE = 1–2 cm). Additional comparison with a salinity-inferred lake level curve showed similar seasonal and interannual variability. The final, pressure-based lake level time series was then adjusted upward by an absolute constant of 2 cm to match the staff gauge measurements.

2.7.3. Latent and sensible heat fluxes

One of the challenges in using the BREB method is the occasional occurrence of Bowen ratios near −1 (Eq. (2)), which can yield unrealistically large estimates of evaporation (or condensation). Previous studies have suggested the use of fixed intervals within which data are discarded, such as $B < -0.75$ or $-1.3 < B < -0.7$ (Ortega-Farias et al., 1996; Unland et al., 1996). This can result, however, in a significant loss of data (Gavilán and Berengena, 2006; Ohmura, 1982; Unland et al., 1996). Others have proposed defining intervals according to the vapor pressure gradient and temperature accuracy (Ohmur, 1982; Perez et al., 1999). Another inherent difficulty with the BREB method is the potentially large uncertainties that can arise in the heat storage term – particularly in deep lakes, where short-term changes in lake temperature (e.g., internal waves) may often be unrelated to the net surface heat flux. Although Alkali Lake is a shallow, well-mixed lake in a windy environment, occasional errors in the heat storage term are certainly possible on short timescales. And in a few rare instances, extremely low water levels were observed at Alkali Lake, causing the lakebed to nearly dry up. This led to considerable errors in the assumed "wet" surface temperature (e.g., dry sand skin temperatures exceeding 40 °C), Bowen ratio, and some energy budget components.

To address the above challenges in *H* and *E* error identification and outlier removal, we used the daily-mean MT estimates of sensible and latent heat flux (Eqs. (11) and (12)) to identify outliers in the BREB-derived estimates of daily *H* and *LE* (Eqs. (2) and (3)). This approach takes advantage of the fact that MT-based estimates of *H*

Table 2
Final regressions and mass-transfer equations for *LE* and *H* (y), determined from the mass transfer products of wind speed and vapor pressure/temperature gradients (x). The independent variables (x) are in units of kPa for *LE* (i.e., vapor pressure gradient) and °C for *H* (i.e., temperature gradient).

	Regression Eq.	R^2	p-value	RMSE
LE	y = 32.9x + 19.8	0.87	<0.0001	21.7 W/m^2
H	y = 2.22x + 0.014	0.97	<0.0001	3.3 W/m^2

and *LE* are not sensitive to errors in the heat storage term, nor instances of *B* approaching −1. The process was iterative, in the sense that egregious outliers were removed first (typically due to $B \approx -1$), followed by a reassessment of the MT coefficients and removal of additional anomalies. The latter step occurred through a careful examination of the top/bottom 5% *H* and *LE* outliers (40 days of data each), including a determination of which method was in error (i.e., BREB or MT), based on values of *B*, the heat storage term, and ambient meteorological and lake conditions. The most appropriate method was then used for the final values of sensible and latent heat flux (Table 2). In cases where the BREB-derived values were replaced with MT estimates (21 instances for *LE*; 39 instances for *H*), the energy budget was also adjusted to balance (i.e., by calculating the rate of heat storage as a residual, rather than using the measured ΔS).

Of the 40 days identified in the above QA/QC procedure, 19 instances were deemed to have indeterminate sources of error in the latent heat flux estimates (i.e., neither the BREB nor MT approach were objectively deemed "best"). In such instances, a hybrid approach was used, which takes advantage of the fact that the MT-derived sensible heat flux values have considerably less uncertainty (RMSE = 3.3 W/m^2) than the MT-derived latent heat flux values (RMSE = 21.7 W/m^2). In this approach, we simply assume the MT-derived *H* to be correct and then calculate the latent heat flux as a residual from the energy balance (using observed heat storage rates). Subsequent "corrected" values of the Bowen ratio were also calculated. In most (but not all) instances where the hybrid approach was implemented, the final value of *LE* was found to be intermediate between the BREB and MT estimates.

3. Results and discussion

3.1. Climate variability

Summer-mean (JAS) climate data from the Alliance North station are shown in Fig. 2 for the 25-year period 1989–2013. Mean JAS air temperature ranges from 17.0 °C (1993) to 21.6 °C (1989), with a long-term average of 19.7 °C. Relative humidity and wind

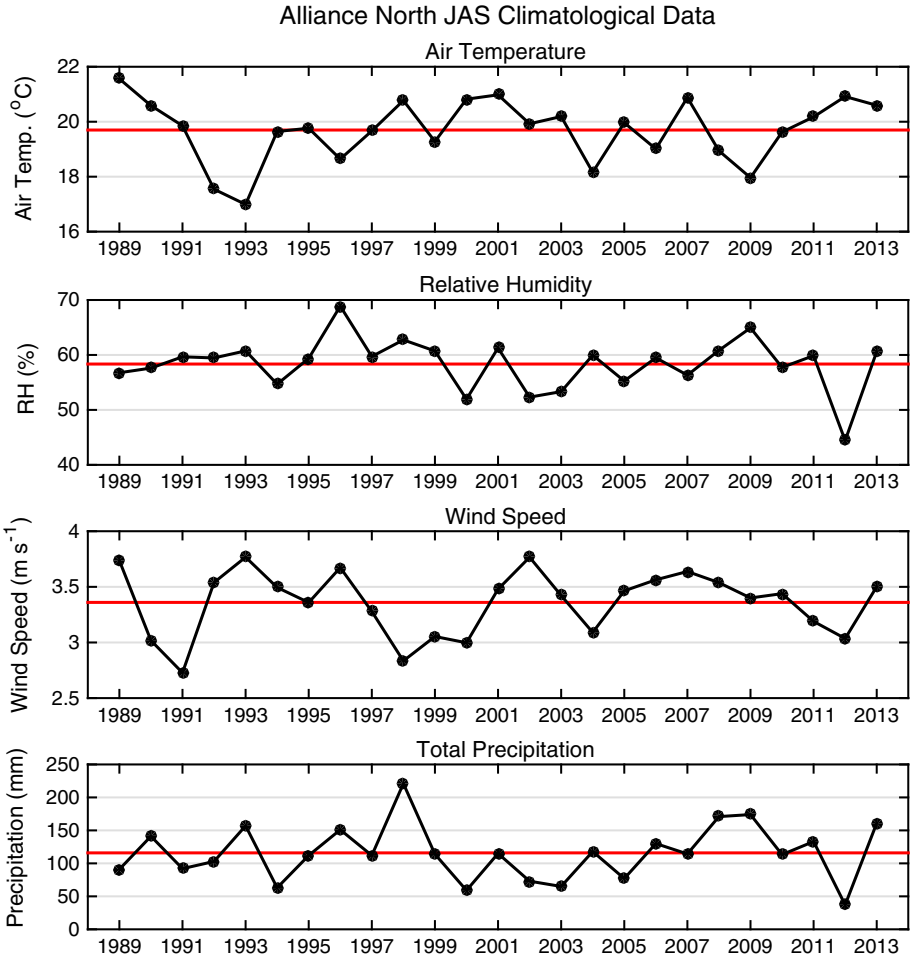

Fig. 2. JAS averages of climatological data from Alliance North, an AWDN station located ~50 km from Alkali Lake. Top to bottom: Air temperature, relative humidity, wind speed, and total JAS precipitation. Red lines indicate the 25-year average, while highlighted blue sections delineate the primary study period (2007–2009).

speed averaged 58% and 3.4 m s^{-1}, respectively, during the 25-year period. Summer-mean precipitation was highly variable, ranging from 37 mm in 2012 to 221 mm in 1998, with a mean value of 120 mm. Given the range of variability in the 25-year record, none of the three summers that are the focus of this study (2007–2009) would be considered particularly anomalous compared to the long-term mean. It is also worth noting that the JAS period is generally warmer, drier, and less windy than the annual average (data not shown), and JAS precipitation can range from 21 to 61% of the annual total (with a mean of 39%).

3.2. Lake energy balance and meteorological drivers

The range of daily values in the JAS Alkali Lake energy balance is illustrated in Fig. 3, which shows histograms for the complete 276-day period (JAS; 2007–2009). Latent heat fluxes range from near zero to above 300 Wm^{-2} (a 10.5 mm day^{-1} evaporation rate), with mean and median values around 145 Wm^{-2} (5.1 mm day^{-1}). In contrast, sensible heat fluxes are largely distributed around zero, with a much smaller standard deviation (19 Wm^{-2}) than *LE* (49 Wm^{-2}). The distribution of daily-mean net radiation values is similar to that of evaporation, with a difference in mean values of only 5 W m^{-2}. Maximum values of R_{net} are somewhat lower than *LE*, however, suggesting additional meteorological drivers of evaporation than R_{net} alone. The total rate of heat storage in the lake (water plus sediments) shows a relatively narrow distribution very similar to that of sensible heat flux, with a mean value near zero. Roughly 45% of the daily observations of *S* and *H* both fall within a range of −10 to +10 W m^{-2}.

Histograms of daily mean air temperature, water-air temperature difference (ΔT), relative humidity, and wind speed from the Alkali Lake buoy measurements (2007–2009) are shown in Fig. 4, highlighting the large daily variability present in this region. Air temperature averaged around 19.8 °C, which is nearly identical to the long-term mean from the Alliance North station. Lake surface temperatures were slightly warmer than air temperature, on average (mean ΔT = 0.8 °C), but with considerable day-to-day variability (range of −6 to +6 °C; standard deviation of 2.0 °C). The distribution of daily mean relative humidity reflects the dry climate of the region, with a mean value of 65% and only a few instances during which the daily mean relative humidity exceeded 80%. Wind speed shows a somewhat skewed distribution, with a median value of 3.6 m s^{-1} and a standard deviation of 1.5 m s^{-1}. Very few days had mean wind speeds below 2 m s^{-1}, indicative of the generally windy environment in the Nebraska Sandhills.

3.3. Seasonal variability in the Alkali lake energy balance

Bi-weekly intervals from May 12 to November 4 were used to illustrate the overall seasonal variability in the Alkali Lake energy balance (Fig. 5). Results are shown beyond the usual JAS period to better capture seasonal variations during late spring and early

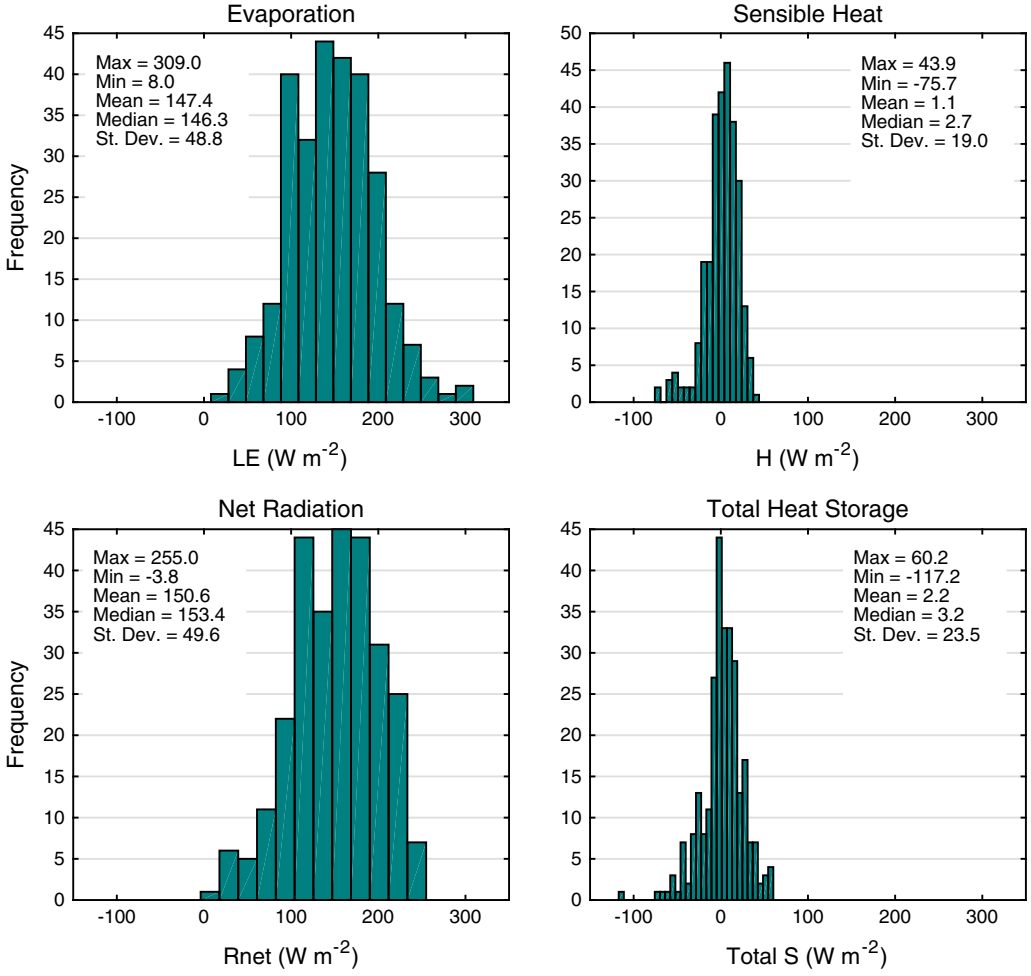

Fig. 3. Histograms of daily energy balance components at Alkali Lake for the JAS period (2007–2009). Top Left: Latent heat flux. Top Right: Sensible heat flux. Bottom Left: Net radiation. Bottom Right: Total rate of heat storage. All measurements are expressed in W m^{-2}.

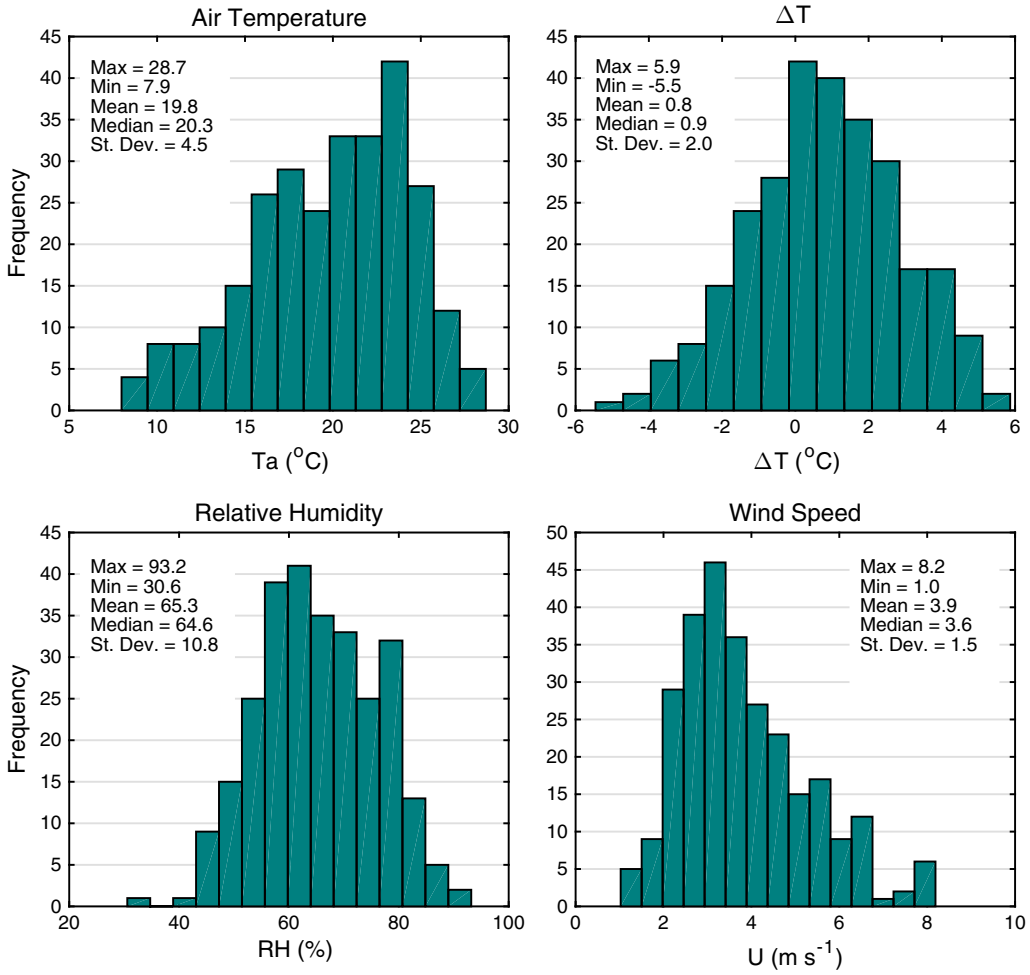

Fig. 4. Distribution of daily mean meteorological data during the JAS period (2007–2009). Top left: Air temperature. Top right: Water-air temperature difference. Bottom left: Relative humidity. Bottom right: Wind speed.

autumn (although not all years had available data in May, June, and October). Similar to the large distribution of daily values (Fig. 3), both latent heat flux and net radiation show considerable seasonal variability, with similar timing and magnitude (Fig. 5). *LE* and R_{net} both peak in late June (~200 W m^{-2}) and gradually decrease to less than 50 W m^{-2} by late October. This is consistent with nearby studies of shallow wetlands (Burba et al., 1999; Parkhurst et al., 1998), and largely a reflection of the energy available to evaporation in mid-summer, particularly for shallow lakes (Brutsaert, 1982). Considerable day-to-day variability in *LE* and R_{net} was observed within most of the bi-weekly periods – particularly for *LE*, which has many large daily values that are not similarly reflected in R_{net}. As noted previously (Fig. 3) this points to high rates of evaporation that are supported not only by R_{net}, but also by the release of stored energy in the lake itself (Fig. 5d).

In contrast to *LE*, no clear seasonal cycle is seen in sensible heat flux, and only a weak signal is evident in the heat storage rate (positive in May and June; slightly negative by September). Both characteristics are indicative of the shallow nature of Alkali Lake, with most of the seasonal cycle in *S* being associated with sediment heat flux. Despite the weak seasonal cycles, both *H* and *S* show considerably larger day-to-day variability (Fig. 5). Maximum and minimum values of *H* are 66 W m^{-2} and −105 W m^{-2}, respectively, with an overall mean of 2 W m^{-2}. Daily heat storage rates also vary greatly (particularly in the spring and fall), with a maximum of 170 W m^{-2} and a minimum of −124 W m^{-2}. Summertime values show a more limited range of variability.

A similar bi-weekly analysis of meteorological data and lake temperature drivers is shown in Fig. 6 in order to more clearly relate climatic drivers to lake heat fluxes (Fig. 5), as well as cross-validate results of the BREB and mass transfer analyses. Fig. 6 includes bi-weekly summaries of daily mean $U(e_s - e_a)$, $U(T_s - T_a)$, $(e_s - e_a)$, and T_s, as well as wind speed and relative humidity. (As noted previously, diurnal covariances are explicitly included in the daily means of the various cross products.) As would be expected from the MT relationship, the seasonal variability in *LE* (Fig. 5) is roughly matched by similar variability in $U(e_s - e_a)$ and even $(e_s - e_a)$ alone (Fig. 6), which also follows the seasonal pattern in lake surface temperature. Much like sensible heat flux (Fig. 5), on the other hand, very little seasonal variability is evident in $U(T_s - T_a)$, due to T_s generally being very similar to T_a, on average.

Wind speed and relative humidity both show less pronounced but still notable seasonal patterns (Fig. 6e-f), with slightly calmer, drier conditions in July and early August and windier, but more humid conditions in spring and autumn. Similar to the results of Lenters et al. (2005), the seasonal wind pattern reflects the influence of midlatitude weather systems, which tend to be more active in spring and fall. It also suggests that lake evaporation rates in mid summer are lower than they would be if wind speeds were more constant throughout the year.

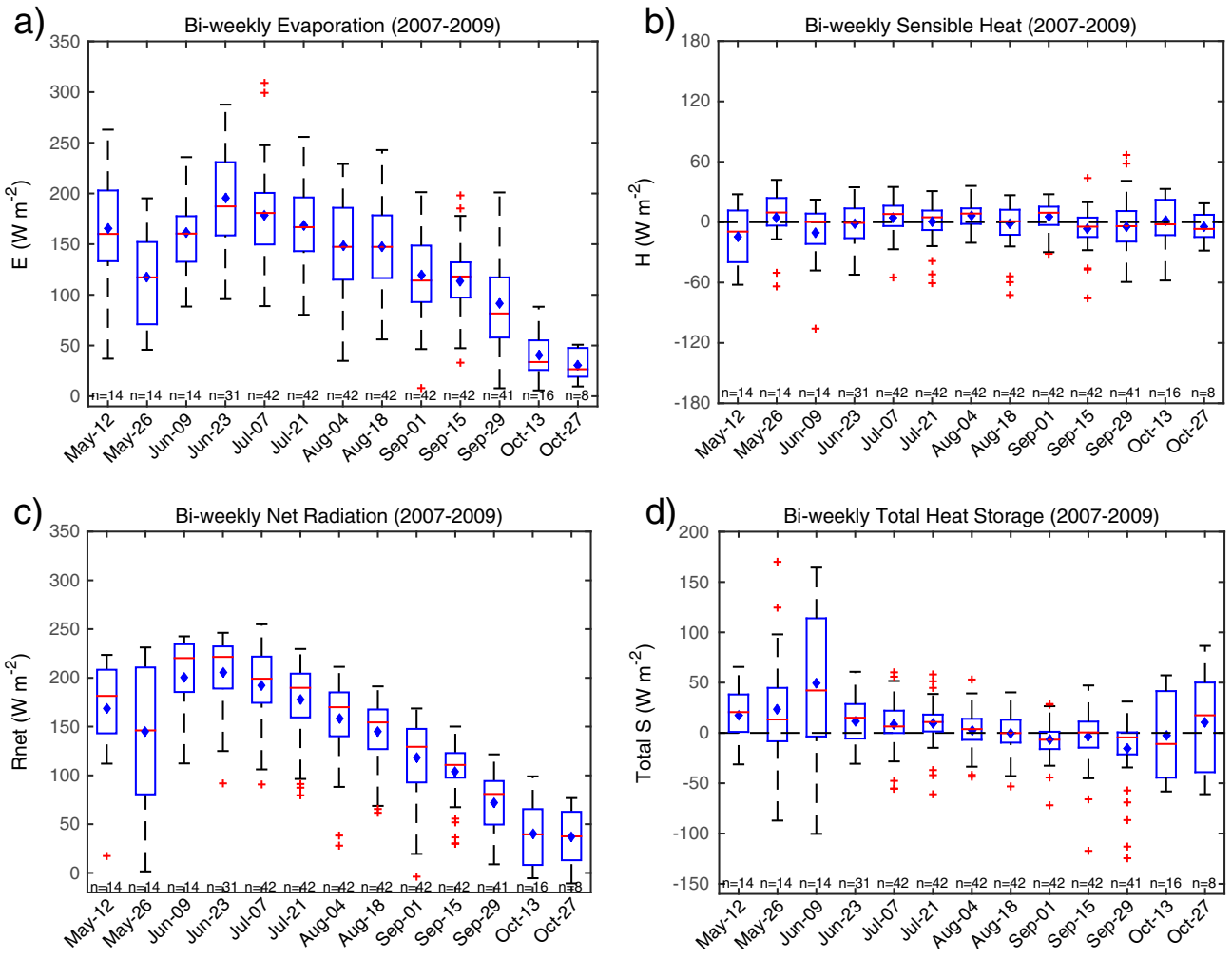

Fig. 5. Seasonal patterns in the various energy balance components for 2007–2009, as depicted by bi-weekly box-and-whisker plots, including a) latent heat flux, b) sensible heat flux, c) net radiation, and d) total rate of heat storage. Blue dots (red lines) represent the mean (median), "+" symbols are outliers, and blue boxes denote the interquartile range. All units are in W m^{-2} and n-values at the bottom denote the total number of days included in a given 2-week period. Each date represents the beginning of a two-week period.

3.4. Interannual variability in the lake energy balance

Interannual variability in the JAS energy balance of Alkali Lake is shown in Fig. 7, along with related climatic parameters in Fig. 8. Although it is clear that many of the interannual changes in the mean energy balance are vastly outweighed by daily and seasonal variations, a few exceptions can be noted. Lake level, for example, increased markedly from 2007 to 2009 (Fig. 7e), and the additional water storage in the lake is reflected in a much more variable heat storage term in 2009 (Fig. 7d), with almost no change in sediment heat flux (Fig. 7f). Higher lake levels in 2009 may also be associated with changes in other temperature-dependent terms. For example, JAS sensible heat fluxes in 2009 were ~19 W m^{-2} higher than in 2007 (Fig. 7b; Table 3), which is much larger than the uncertainty in the measurements themselves. This suggests that the lake retained greater amounts of energy, creating a larger temperature differential with the atmosphere and greater fluxes of sensible heat. This is borne out by observations of $U(T_s - T_a)$ and $(T_s - T_a)$, both of which were considerably larger in 2009 compared to the previous two years (Fig. 8; Table 4). Additional years of observations would be needed to fully assess the effects of lake level variability on water temperature and the heat storage term, since seasonal and (especially) daily variations in lake level are generally too weak to adequately define a relationship.

Similar to the 19 W m^{-2} increase in sensible heat flux, *LE* showed a decline of ~14 W m^{-2} from 2007 to 2009 (Fig. 7a; Table 3). Although this difference is within the bounds of uncertainty in *LE*, it implies a potential compensatory relationship between *H* and *LE*, as R_{net} showed essentially no change from 2007 to 2009 (Fig. 7c; Table 3). In other words, the reduction in evaporative cooling may have contributed to warmer lake surface temperatures (relative to air) and an associated increase in sensible heat flux.

3.5. Influence of salinity on mass transfer and energy balance results

Similar to lake level, the absolute salinity of Alkali Lake varied widely over the 3-year period, ranging from 118.5 g kg^{-1} in August of 2007 to 28.5 g kg^{-1} in July of 2009 (Fig. 9), corresponding with large (but opposing) changes in lake level. Despite the large changes in salinity, the effect on activity coefficient was found to be relatively small, with most values being only 2–6% less than the freshwater value of 1.0 (Fig. 9). Although this might suggest a similarly negligible impact on the resulting lake evaporation estimates, this turns out not to be the case in all instances. To illustrate this, we further examined the effects of fluctuating salinity on the mass transfer (Eq. (11)) and BREB-derived (Eq. (2)) estimates of latent heat flux by recalculating *LE* assuming freshwater metrics,

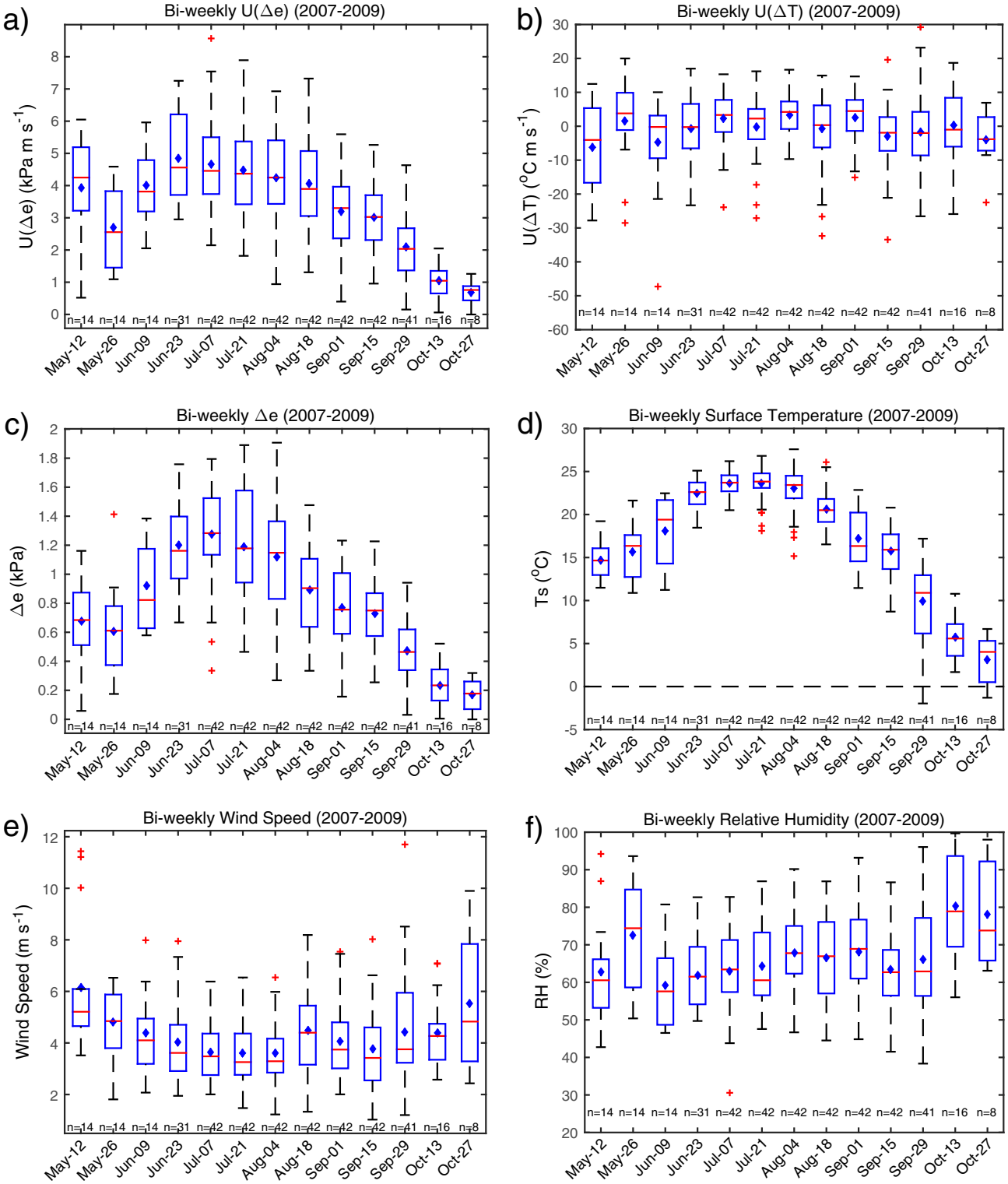

Fig. 6. Seasonal patterns in the various meteorological components for 2007–2009, as depicted by bi-weekly box-and-whisker plots, including a) the product of wind speed and vapor pressure gradient (kPa m s^{-1}), b) the product of wind speed and temperature gradient (°C m s^{-1}), c) vapor pressure gradient (kPa), d) temperature gradient (°C), e) wind speed (m s^{-1}), and f) relative humidity (%). Blue dots (red lines) represent the mean (median), "+" symbols are outliers, and blue boxes denote the interquartile range. n-values at the bottom denote the total number of days included in a given two-week period.

rather than the observed saline values. This included not only changes in the activity coefficient (a_w = 1 for fresh water), but also changes in the density and specific heat of water. Fig. 10 shows how variations in *aw* propagate from roughly 2–6% changes in daily mean e_s to ~0–20% changes in mass transfer estimates of daily $U(e_s - e_a)$ and the associated latent heat flux (~0–30 W m^{-2}). These results indicate that small changes in *aw* can occasionally translate into much larger changes in daily lake evaporation, such as on humid days when e_a is close to e_s (i.e., resulting in a larger percent change in $e_s - e_a$ than e_s alone).

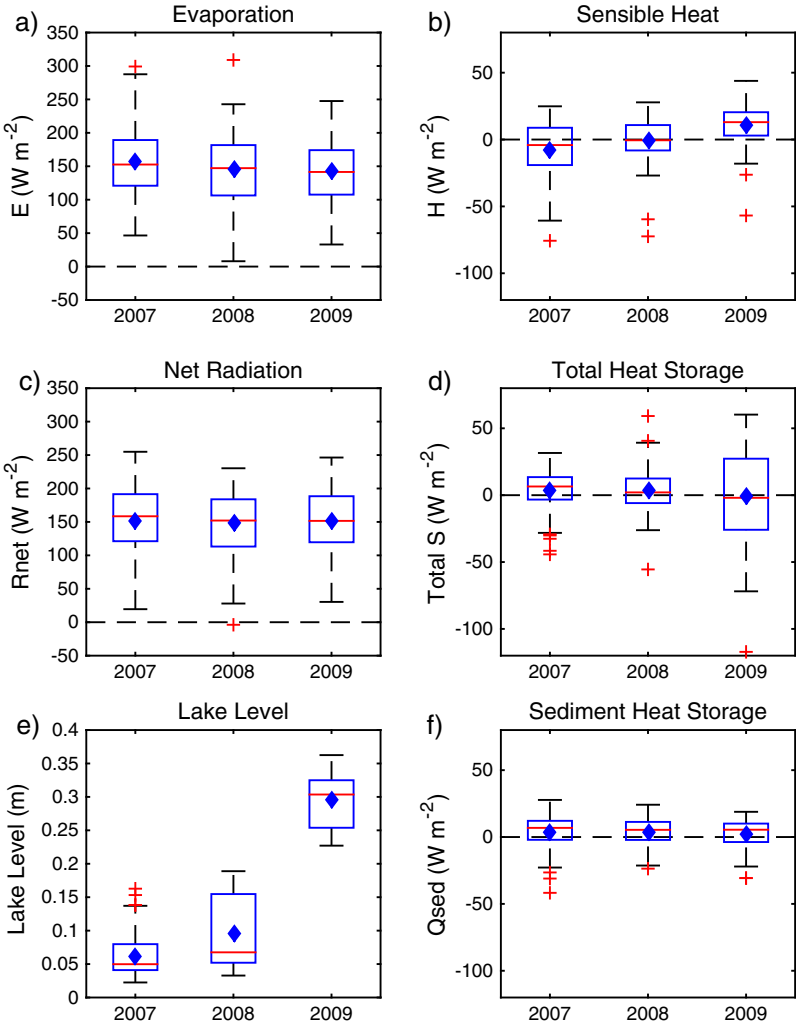

Fig. 7. Box-and-whisker plots illustrating the interannual variability between the three JAS periods from 2007 to 2009. Shown is the a) latent heat flux (W m^{-2}), b) sensible heat flux (W m^{-2}), c) net radiation (W m^{-2}), d) total rate of heat storage (W m^{-2}), e) lake level (m), and f) rate of heat storage in the sediments (W m^{-2}). Blue dots represent averages for that year, red lines are medians, and "+" symbols indicate outliers.

The effects of salinity on BREB-derived evaporation rates are slightly more complicated, since salinity variations affect *LE* not only through the Bowen ratio (via changes in a_w), but also through the water heat storage term (via changes in water density and specific heat). Fig. 11 illustrates these changes and the effect on BREB-derived *LE* values. Water heat storage rates change relatively little, with a median value near zero and a range of roughly +/−2 W m^{-2}, or +/−5% (Fig. 11a-b). Changes in Bowen ratio, however, are more prominent, with a median change of ~0, but a range of roughly +/−20% (Fig. 11c-d). As with the mass transfer results, some of these larger percent changes in *B* are due to changes in e_s that lead to larger percent changes in $e_s - e_a$. Although these variations can get further amplified when calculating *LE* (e.g., when *B* approaches −1), instances of this were not found to be common, since *B* values for Alkali Lake are commonly near 0. Furthermore, unlike the mass transfer results, BREB-derived values of *LE* are constrained by the amount of available energy, with *B* affecting the partitioning between *H* and *LE* (i.e., not just the magnitude of *LE* alone). As a result, the effect of salinity changes on BREB-derived values of *LE* tend to be smaller than those of the mass transfer method, and generally within about +/−5% (Fig. 11e-f). Furthermore, the salinity effects on BREB-derived *LE* have a mean bias of ~0, unlike the negative bias of 0–20% seen previously for the mass transfer method (Fig. 10e-f). The results of this analysis indicate that BREB-based estimates of lake evaporation are less sensitive to the impact of salinity than mass transfer estimates and, therefore, are a more robust technique to use when absolute salinity is poorly quantified or even unknown (e.g., assumed fresh water). On the other hand, considerable caution must be exercised when using even the BREB estimates of *LE* to calibrate a mass transfer approach, since the latter is much more sensitive to the effects of salinity and would, therefore, require accurate values of absolute salinity to be appropriately calibrated.

4. Summary and conclusions

Alkali Lake is a characteristically shallow, saline lake in the Sandhills region of western Nebraska. The Sandhills are located in a warm, windy, semi-arid environment with numerous groundwater-fed, endorheic or poorly draining lakes, making it an excellent laboratory for field studies of open-water evaporation. This study has examined the seasonal and interannual variability in lake evaporation over a 3-year period using the Bowen ratio energy balance method. Calculations of latent and sensible heat flux using the mass transfer technique were also employed to aid in the QA/QC process of the BREB-derived results. Data were collected during the warm-season months of May – October, with

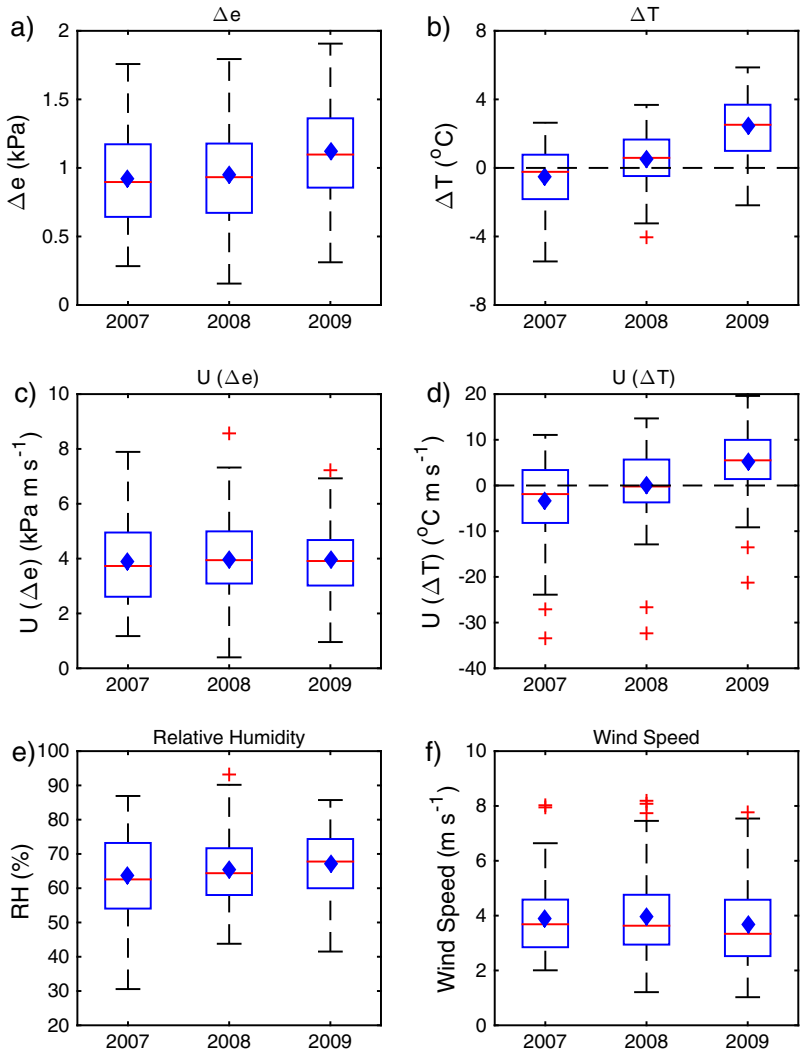

Fig. 8. Box-and-whisker plots illustrating the interannual variability between the three JAS periods from 2007 to 2009. Shown is the a) vapor pressure difference (kPa), b) temperature gradient (°C), c) product of wind speed and vapor pressure difference (kPa m s^{-1}), d) product of wind speed and temperature gradient (°C m s^{-1}), e) relative humidity (%), and f) wind speed (m s^{-1}). Blue dots represent averages for that year, red lines are medians, and "+" symbols indicate outliers.

Table 3
Mean JAS values for each component of the energy balance, along with their estimated uncertainty (based on assumed instrument error). All units are in W m^{-2}.

	LE	*H*	R_{net}	*S* (water)	*S* (total)	Q_{sed}
2007	155.9	−7.7	152.1	0.1	3.9	3.8
2008	144.6	−0.3	148.2	0.0	3.9	3.9
2009	141.7	11.2	151.6	−3.8	−1.3	2.5
Uncertainty	±21.6	±3.4	±25.7	±10.0	±10.2	±2.0

Table 4
Mean JAS values of lake and atmospheric variables for each year, along with the estimated uncertainty (based on assumed instrument error).

	$T_s - T_a$ (°C)	$e_s - e_a$ (kPa)	$U(e_s - e_a)$ (kPa m s^{-1})	$U(T_s - T_a)$ (°C m s^{-1})	U (m s^{-1})	RH (%)	Lake level (m)
2007	−0.5	0.93	3.9	−3.4	3.9	63.5	0.06
2008	0.5	0.95	4.0	−0.1	4.0	65.5	0.10
2009	2.4	1.12	4.0	5.3	3.7	67.1	0.30
Uncertainty	±0.7	±0.4	±3.4	±4.3	±0.5	±5.0	±0.03

the most complete, 3-year dataset comprised of the months of July, August, and September (JAS). Daily mean evaporation rates at Alkali Lake were found to reach their seasonal peak in late June and early July, averaging around 7.0 mm day^{-1}, with a maximum daily mean evaporation rate of 10.5 mm day^{-1}. The 3-year mean evaporation rate at Alkali Lake for the 3-month JAS period was found to be 5.1 mm day^{-1}, which greatly exceeds the long-term mean JAS precipitation rate of 1.3 mm day^{-1} measured at a nearby long-term weather station. This implies an average net loss of water from the lake of roughly 0.35 m over the course of the

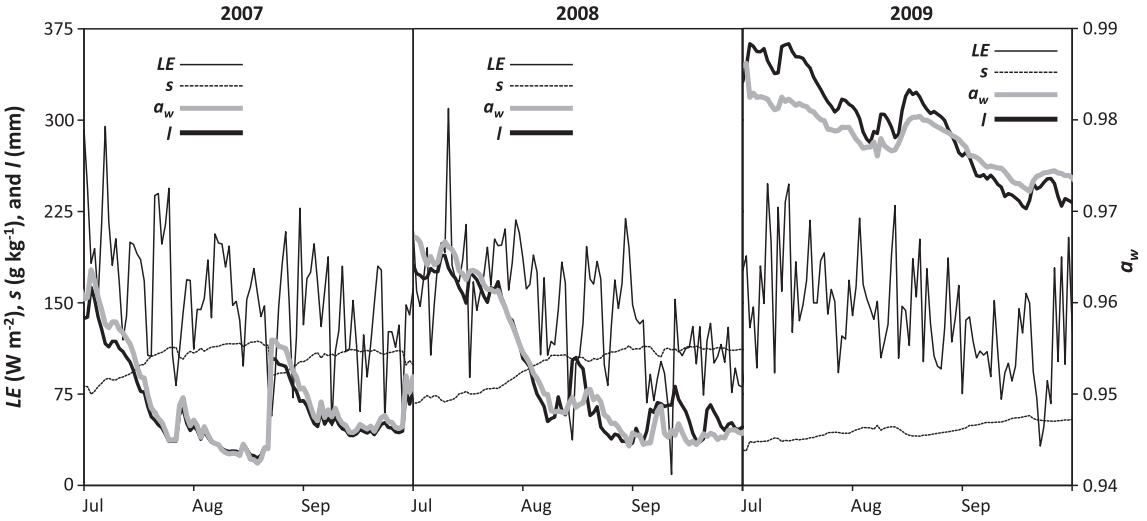

Fig. 9. July-September daily mean lake level, absolute salinity, and activity coefficient (a_w) for Alkali Lake during the period 2007–2009.

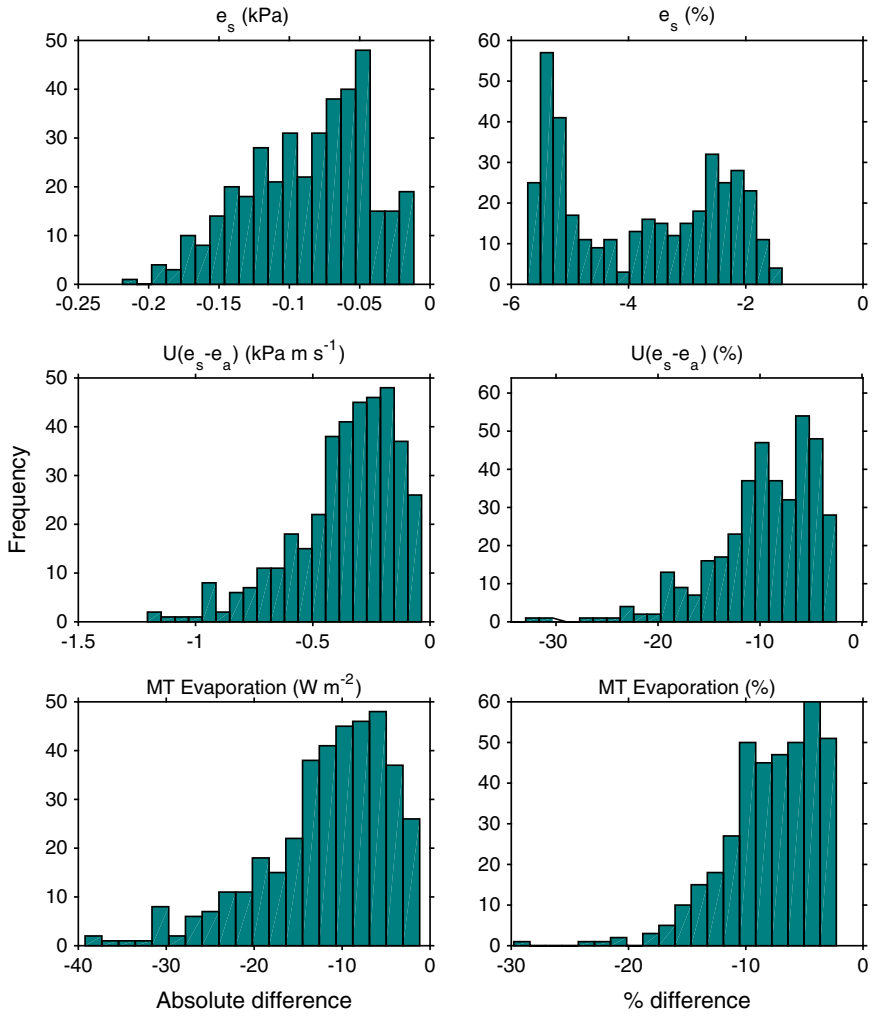

Fig. 10. Absolute (a, c, e) and percent differences (b, d, f) of surface vapor (a, b), mass transfer product (c, d), and mass transfer evaporation (e, f). Not all outliers are shown.

92-day JAS period, which is more than the typical drop in lake level observed during that time of year, implying compensatory inputs from groundwater.

Seasonal variations in evaporation at Alkali Lake were found to be considerably larger than interannual variations, with the seasonal variability in *LE* closely matching that of net radiation

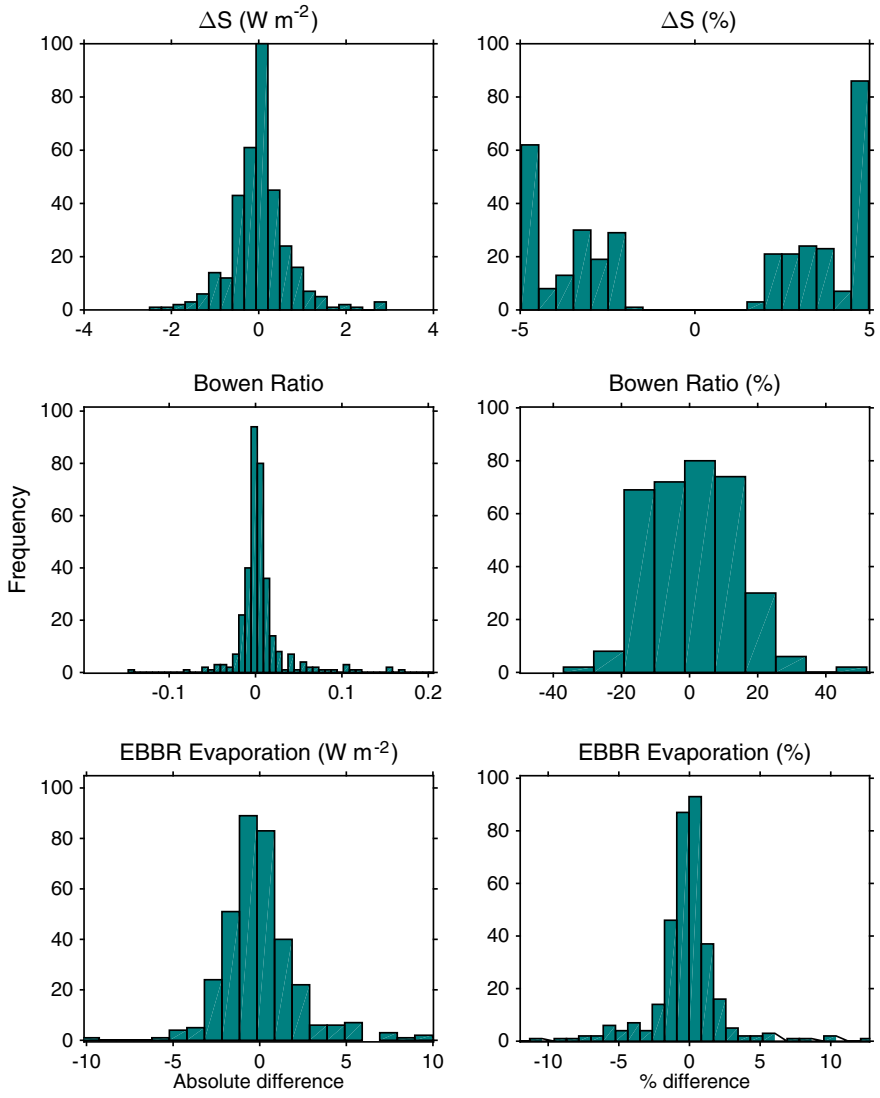

Fig. 11. Absolute (a, c, e) and percent differences (b, d, f) of water heat storage (a, b), Bowen ratio (c, d), and energy balance evaporation rates (e, f). Not all outliers are shown.

(e.g., peaking in late June, with considerable decline into autumn). This is consistent with studies of shallow freshwater wetlands in the region (Burba et al., 1999; Parkhurst et al., 1998) and is also a common finding of wetlands in general (Brutsaert, 1982). Seasonality in other meteorological variables is also evident at Alkali Lake, with the mass transfer product of wind speed and vapor pressure gradient closely matching that of evaporation. This shows the potential merit for using the less costly and time-consuming mass transfer method in estimating seasonal evaporation rates at Alkali Lake in future studies, so long as salinity is appropriately accounted for in the vapor pressure gradient. Alkali Lake also displayed other characteristics similar to those generally observed in shallow lakes, such as relatively low mean values of sensible heat flux and rates of heat storage in the water and sediments, as well as limited seasonal variability in both terms (relative to net radiation and latent heat flux). Despite the overall weak contributions from sensible heat flux and internal heat storage (on average), however, it is important to note that occasionally large daily mean values (100–150 W m^{-2}) were found to occur in both of these components in association with synoptic weather variability. Thus, although seasonal variations in net radiation largely determine the mean seasonal cycle of latent heat flux, transient weather events introduce significant contributions from sensible heat flux and the storage / release of heat from the lake water and sediments.

Although Alkali Lake exhibits a fairly pronounced seasonal cycle in evaporation, the large daily variability that was observed suggests that no two years are identical, in terms of their overall, seasonal pattern. Similar conclusions have been reached in other multi-year lake evaporation studies, where it has been noted that large intraseasonal variation can cause daily conditions during individual years to be very different from the long-term average (Parkhurst et al., 1998, Lenters et al., 2005). It should also be noted that although large variations in lake level and salinity at Alkali Lake translated into relatively small variations in the activity coefficient of water, properly accounting for the role of salinity resulted in a moderate reduction in evaporation rates (up to 10–20%) when calculated via the mass transfer technique. BREB-derived estimates of evaporation, on the other hand, were found to be less sensitive to the role of salinity (+/−5%) due to energy balance constraints and contributions from changes in the density and specific heat of saline water.

Interannual variability in the JAS latent heat flux and evaporation rate at Alkali Lake is small, with mean differences between years being less than 15 W m^{-2} (0.5 mm day^{-1}), which is well within the estimated uncertainty of 22 W m^{-2} in the BREB method.

Similar conclusions were reached for net radiation, but not sensible heat flux and the associated lake-air temperature gradient, both of which showed increases from 2007 to 2009 that exceeded the measurement uncertainty (Table 3). This was accompanied by progressively larger variations in heat storage rate from 2007 to 2009, and we attribute all of these latter effects to the overall increase in lake level observed over the three-year period. In other words, the transition of Alkali Lake from a 5-cm "pond" in 2007 to a 30-cm deep "lake" in 2009 resulted in greater internal storage of heat, an increasing lag between variations in air and water temperature, and – as a result – generally higher water temperatures than air temperature, with correspondingly higher sensible heat fluxes. The latter effects are reminiscent of deeper lakes, but they have been observed at the smaller scale of Alkali Lake, despite what might otherwise be considered inconsequential changes in water level. Additional years of analysis would be helpful for further elucidating the influence of large changes in water level on the lake energy balance.

The results of this study have important implications for the estimation and understanding of the warm-season water balance of saline lakes in arid and semi-arid regions. The high evaporation rates at Alkali Lake substantially exceed the local precipitation rate, implying an important role from groundwater in contributing water and solutes. Given the significance of the Nebraska Sandhills region as an important recharge zone for the supply of irrigation and drinking water in one of the most agriculturally productive regions of the world, the information provided in this study is timely and relevant. We anticipate that the results presented here will help to characterize the primary drivers of the energy, water, and solute balance of saline lakes and wetlands across the Nebraska Sandhills and similar regions of the world, thereby contributing to improved estimates of evaporation and recharge rates for aquifers in semi-arid landscapes.

Acknowledgments

This work was funded by the Department of Geography at the University of North Carolina at Chapel Hill and by the Agricultural Research Division at the University of Nebraska-Lincoln. Two reviewers and the associate editor provided valuable suggestions for the improvement of this manuscript.

References

Abbo, H., Shavit, U., Markel, D., Rimmer, A., 2003. A numerical study on the influence of fractured regions on lake/groundwater interaction; the Lake Kinneret case. J. Hydrol. 283 (1–4), 225–243.

Befus, K., Cardenas, M.B., Ong, J.B., Zlotnik, V.A., 2012. Classification and delineation of groundwater – lake interactions in the Nebraska Sand Hills (USA) using quasi-3D electrical resistivity surveys. Hydrogeol. J. 20 (8), 1483–1495. http://dx.doi.org/10.1007/s10040-012-0891-x, 2012.

Billesbach, D.P., Arkebauer, T.J., 2012. First long-term, direct measurements of evapotranspiration and surface water balance in the Nebraska SandHills. Agric. For. Meteorol. 156, 104–110. http://dx.doi.org/10.1016/j.agrformet.2012.01.001.

Blanken, P. D., Rouse, W. R., Culf, A. D., Spence, C., Boudreau, D. L., Jasper, J. N., et al. (2000). Eddy covariance measurements of evaporation from Great Slave lake, Northwest Territories, Canada. Wat. Resour. Res., 36(4), 1069–1077. Retrieved from http://research.eeescience.utoledo.edu/lees/LESensorN/Refs%5CPapersinLakefluxstudies%5CBlanken2000.pdf.

Blanken, P.D., Spence, C., Hedstrom, N., Lenters, J.D., 2011. Evaporation from Lake Superior: 1. Physical controls ans processes. J. Great Lakes Res. 37 (4), 707–716.

Bleed, A., & Flowerday, C. (Eds.). (1998). An Atlas of the Sand Hills (3rd ed.).

Brutsaert, W., 1982. Evaporation into the Atmosphere: Theory, History, and Applications. D. Reidel, Dordrecht, Holland.

Burba, G., Verma, S., Kim, J., 1999. Energy fluxes of an open water area in a mid-latitude prairie wetland Retrieved from Bound.-Layer Meteorol., 495–504

Chen, X., Hu, Q., 2004. Groundwater influences on soil moisture and surface evaporation. J. Hydrol. 297 (1–4), 285–300. http://dx.doi.org/10.1016/j.jhydrol.2004.04.019.

dos Reis, R., Dias, N., 1998. Multi-season lake evaporation: energy-budget estimates and CRLE model assessment with limited meteorological observations Retrieved fromhttp://www.sciencedirect.com/science/article/pii/S0022169498001607 J. Hydrol. 208, 135–147.

Drexler, J.Z., Snyder, R.L., Spano, D., Paw, U.K.T., 2004. A review of models and micrometeorological methods used to estimate wetland evapotranspiration. Hydrol. Process 18 (11), 2071–2101. http://dx.doi.org/10.1002/hyp.1462.

Evans, J.P., Oglesby, R.J., Lapenta, W.M., 2005. Time series analysis of regional climate model performance. J. Geophys. Res. 110 (D4). http://dx.doi.org/10.1029/2004JD005046.

Garrels, R., Christ, C., 1965. Solutions, minerals, and equilibria. Harper and Row, San Francisco, p. 450.

Gavilán, P., Berengena, J., 2006. Accuracy of the Bowen ratio-energy balance method for measuring latent heat flux in a semiarid advective environment. Irrig. Sci. 25 (2), 127–140. http://dx.doi.org/10.1007/s00271-006-0040-1.

Hage, K., 1975. Averaging errors in monthly evaporation estimates Retrieved from Water Resour. Res. 11 (2), 359–361.

Healey, N.C., Irmak, A., Arkebauer, T.J., Billesbach, D.P., Lenters, J.D., Hubbard, K.G., Kjaersgaard, J., 2011. Remote sensing and in situ-based estimates of evapotranspiration for subirrigated meadow, dry valley, and upland dune ecosystems in the semi-arid sand hills of Nebraska, USA. Irr. Drain. Syst. 25 (3), 151–178. http://dx.doi.org/10.1007/s10795-011-9118-x.

Jobson, H., 1972. Effect of using averaged data on the computed evaporation Retrieved from Water Resour. Res. 8, 513–518.

Keshari, A., Koo, M., 2007. A numerical model for estimating groundwater flux from subsurface temperature profiles. Hydrol. Process. 3448, 3440–3448. http://dx.doi.org/10.1002/hyp.

Kondo, J., 1972. Applicability of micrometeorological transfer coefficient to estimate the long-period means of fluxes in air–sea interface Retrieved from J. Meteor. Soc. Japan 50 (6), 570–576.

Langbein, W.B. (1961). Salinity and hydrology of closed lakes. USGS Professional Paper 412, pp. 20. Washington, U.S. Govt. Print. Off.

Lee, T., Swancar, A., 1997. Influence of evaporation, ground water, and uncertainty in the hydrologic budget of Lake Lucerne, a seepage lake in Polk County, Florida Retrieved from US Geological Survey Water-Supply Paper 2439, 15–28.

Lenters, J.D., Kratz, T.K., Bowser, C.J., 2005. Effects of climate variability on lake evaporation: Results from a long-term energy budget study of Sparkling Lake, northern Wisconsin (USA). J. Hydrol. 308 (1–4), 168–195. http://dx.doi.org/10.1016/j.jhydrol.2004.10.028.

Liu, Y., Hiyama, T., Yasunari, T., Tanaka, H., 2012. A nonparametric approach to estimating terrestrial evaporation: Validation in eddy covariance sites. Agric. For. Meteorol. 157, 49–59. http://dx.doi.org/10.1016/j.agrformet.2012.01.012.

Loope, D., Swinehart, J., Mason, J., 1995. Dune-dammed paleovalleys of the Nebraska Sand Hills: intrinsic versus climatic controls on the accumulation of lake and marsh sediments Retrieved from Geol. Soc. Am. Bull. 107 (4), 396–406.

McCarraher, D. (1977). Nebraska's Sandhills Lakes. Nebraska Game and Parks Commission.

McGloin, R., McGowan, H., McJannet, D., Burn, S., 2014. Modelling sub-daily latent heat fluxes from a small reservoir. J. Hydrol. 519, 2301–2311.

Micklin, P.P. (1992). The Aral Crisis: Introduction to the Special Issue. Post-Soviet Geograph., 33(5), 269–282.

Núñez, C.M., Varas, E.A., Meza, F.J., 2010. Modelling soil heat flux. Theoret. Appl. Climatol. 100 (3–4), 251–260. http://dx.doi.org/10.1007/s00704-009-0185-y.

Ohmura, A. (1982). Objective criteria for rejecting data for Bowen ratio flux calculations. Journal of Applied Meteorology, 21, 595–598. Retrieved from http://journals.ametsoc.org/doi/abs/10.1175/1520-0450(1982)021<0595:OCFRDF>2.0.CO;2.

Ong, J.B.T. (2010) Investigation of spatial and temporal processes of lake-aquifer interactions in the Nebraska sand Hills, Ph.D. Dissertation, University of Nebraska-Lincoln.

Ong, J., Lane, J., Zlotnik, V., Halihan, T., White, E., 2010. Combined use of frequency-domain electromagnetic and electrical resistivity surveys to delineate near-lake groundwater flow in the semi-arid Nebraska Sand Hills, USA. Hydrogeol. J. 18 (6), 1539–1545. http://dx.doi.org/10.1007/s10040-010-0617-x.

Oroud, I., 1997. Diurnal evaporation from fresh and hypersaline shallow ponds in a hot, dry environment Retrieved from Phys. Geogr. 18 (4), 363–382.

Oroud, I.M., 2001. Dynamics of evaporation from saline water bodies. J. Geophys. Res. 106 (D5), 4695. http://dx.doi.org/10.1029/2000JD900061.

Ortega-Farias, S., Cuenca, R., and Ek, M. (1996). Daytime variation of sensible heat flux estimated by the bulk aerodynamic method over a grass canopy. Agricultural and Forest Meteorology, 56(071). Retrieved from http://www.sciencedirect.com/science/article/pii/0168192395022783.

Parkhurst, R., Winter, T., Rosenberry, D., Sturrock, A., 1998. Evaporation from a small prairie wetland in the Cottonwood Lake area, North Dakota—an energy-budget study Retrieved from Wetlands 18, 272–287.

Payne, R. (1972). Albedo of the sea surface. J. Atmos. Sci., 29, 959–970. Retrieved from http://journals.ametsoc.org/doi/abs/10.1175/1520-0469(1972)029%3C0959:AOTSS%3E2.0.CO;2.

Perez, P.J., Castellvi, F., Ibañez, M., Rosell, J.I., 1999. Assessment of reliability of Bowen ratio method for partitioning fluxes. Agric. For. Meteorol. 97 (3), 141–150. http://dx.doi.org/10.1016/S0168-1923(99)00080-5.

Radell, D.B., Rowe, C.M., 2008. An Observational Analysis and Evaluation of Land Surface Model Accuracy in the Nebraska Sand Hills. J. Hydrometeorol. 9 (4), 601–621. http://dx.doi.org/10.1175/2007JHM913.1.

Rimmer, A., Hurwitz, S., Gvirtzman, H., 1999. Spatial and temporal characteristics of saline springs: sea of Galilee, Israel. Ground Water 37 (5), 663–673.

Rimmer, A., Gal, G., 2003. Estimating the saline springs component in the solute and water balance of Lake Kinneret, Israel. J. Hydrol. 284, 228–243.

Rosenberry, D.O., Winter, T.C., Buso, D.C., Likens, G.E., 2007. Comparison of 15 evaporation methods applied to a small mountain lake in the northeastern USA. J. Hydrol. 340 (3–4), 149–166. http://dx.doi.org/10.1016/j.jhydrol.2007.03.018.

Sahagian, D., 2000. Global physical effects of anthropogenic hydrological alterations: sea level and water redistribution Retrieved from Global Planet. Change 25, 39–48.

Salhotra, A., 1985. Effect of salinity and ionic composition on evaporation: analysis of Dead Sea evaporation pans Retrieved from Water Resour. Res. 21, 1336–1344.

Scanlon, Bridget, R., Faunt, Claudia, C., Longuevergne, L., Reedy, Robert, C., & Alley, William, M. (2012). Groundwater depletion and sustainability of irrigation in the US High Plains and Central Valley. USGS Staff – Published Research, Paper 497. Retrieved from http://www.pnas.org/content/109/24/9320.short.

Smith, N., 2002. Observations and simulations of water-sediment heat exchange in a shallow coastal lagoon Retrieved from Estuaries 25 (3), 483–487.

Steenburgh, J. W., Halvorson, S. F., & Onton, D. J. (2000). Climatology of Lake-Effect Snowstorms of the Great Salt Lake. Month. Weather Rev., 128(3), 709–727. Retrieved from http://journals.ametsoc.org/doi/abs/10.1175/1520-0493(2000)128%3C0709%3ACOLESO%3E2.0.CO%3B2.

Tanny, J., Cohen, S., Assouline, S., Lange, F., Grava, A., Berger, D., Parlange, M.B., 2008. Evaporation from a small water reservoir: Direct measurements and estimates. J. Hydrol. 351 (1–2), 218–229. http://dx.doi.org/10.1016/j.jhydrol.2007.12.012.

Unland, H.E., Houser, P.R., Shuttleworth, W.J., Yang, Z. (1996). Surface flux measurement and modeling at a semi-arid Sonoran Desert site, 1923(96).

Webb, E., 1960. On estimating evaporation with fluctuating Bowen ratio Retrieved from J. Geophys. Res. 65, 3415–3417.

Webb, E., 1964. Further note on evaporation with fluctuating Bowen ratio Retrieved from J. Geophys. Res. 69 (12), 2649–2650.

Williams, W.D., 2002. Environmental threats to salt lakes and the likely status of inland saline ecosystems in 2025. Environ. Conserv. 29 (02), 154–167. http://dx.doi.org/10.1017/S0376892902000103.

Winter, T., Buso, D., Rosenberry, D., 2003. Evaporation determined by the energy-budget method for Mirror Lake, New Hampshire Retrieved from Limnol. Oceanograph. 48 (3), 995–1009.

Winter, T.C. (1990). Map distribution of the difference between precipitation and open water evaporation in North America. In Geology of North America, Map GNA-01. Denver, Colorado: U.S. Geological Survey.

Winter, T.C., Rosenberry, D.O., Buso, D.C., Merk, D.A., 2001. Water source to four U.S. wetlands: Implications for wetland management. Wetlands 21 (4), 462–473. http://dx.doi.org/10.1672/0277-5212(2001) 021[0462:WSTFUS]2.0.CO;2.

Zlotnik, V.A., Robinson, N. I., Simmons, C. T., 2010. Salinity dynamics of discharge lakes in dune environments: conceptual model, Water Resour. Res., 46(11) doi: 10.1029/2009WR008999.

Zlotnik, V.A., Ong, J.B., Lenters, J.D., Schmieder, J., Fritz, S.C., 2012. Quantification of salt dust pathways from a groundwater-fed lake: implications for solute budgets and dust emission rates. J. Geophys. Res. 117. http://dx.doi.org/10.1029/2011JF002107.